International Journal of Heat and Mass Transfer 55 (2012) 5205–5213

Contents lists available at SciVerse ScienceDirect

International Journal of Heat and Mass Transfer

journal homepage: www.elsevier.com/locate/ijhmt

Parametric study on turbulent heat transfer and flow characteristics in a circular tube fitted with louvered strip inserts

A.W. Fan [a], J.J. Deng [a], A. Nakayama [b], W. Liu [a,*]

[a] School of Energy and Power Engineering, Huazhong University of Science and Technology, Wuhan 430074, China
[b] Department of Mechanical Engineering, Shizuoka University, 3-5-1 Johoku, Hamamatsu 432-8561, Japan

ARTICLE INFO

Article history:
Received 27 May 2011
Received in revised form 4 April 2012
Accepted 4 May 2012
Available online 7 June 2012

Keywords:
Heat transfer enhancement
Flow resistance
Turbulent flow
Louvered strip inserts
Thermo-hydraulic performance

ABSTRACT

In the present work, characteristics of heat transfer, flow resistance, and overall thermo-hydraulic performance of turbulent airflow in a circular tube fitted with louvered strip inserts were investigated through numerical simulation. Our main attention was paid to the effects of the slant angle and pitch of the turbulators. The results show that the Nusselt number is augmented by 2.75–4.05 times (Nu = 108.71–423.87) as that of the smooth tube. The value of performance evaluation criterion (PEC) lies in the range of 1.60–2.05, which demonstrates that the louvered strip insert has a very good overall thermo-hydraulic performance. Moreover, the computational results indicate that larger slant angle and small pitch can effectively enhance the heat transfer rate, but also increase the flow resistance. Furthermore, it is noted that the Nusselt number and friction factor are more sensitive to the slant angle than the inserts pitch. Comparatively steady and good overall thermo-hydraulic performance can be obtained at a moderate slant angle together with a small pitch. All these data show that the louvered strip is a promising tube insert which would be widely used in heat transfer enhancement of turbulent flow.

1. Introduction

Shell-and-tube heat-exchangers are extensively used in various industrial fields such as petrochemical industry, power generation, air-conditioning, etc. In those devices, heat is transferred from the hot side to the cold side via the tube walls. In cases of low heat transfer rate, additional approaches are necessary to intensify the heat transfer process. Scientists and engineers around the world have made great contributions to heat transfer augmentation techniques [1]. Usually, these techniques are classified either as passive or active. Their major difference is that direct application of external power is not needed for the passive techniques. Thus, they are more frequently adopted in practical applications. Numerous types of turbulators, such as the twisted tape, helical screw-tape, porous media inserts, etc. belong to the passive techniques [2]. The general mechanism of heat transfer enhancement by using tube inserts is that the turbulators can intensify the swirl flow and reduce the thickness of the thermal boundary layer as well. Therefore, heat transfer rate can be augmented. Unfortunately, flow resistance increment is accompanied inevitably. To comprehensively evaluate the overall thermo-hydrodynamic performance of various augmentation methods, many performance evaluation criteria (PEC) have been proposed by different researchers. The one that is most frequently applied is given in Eq. (1) [3],

$$\mathrm{PEC} = \frac{Nu/Nu_0}{(f/f_0)^{1/3}} \tag{1}$$

where Nu and Nu_0 are the Nusselt numbers of the enhanced tube and smooth tube, and f and f_0 are the friction factors of the enhanced tube and smooth tube, respectively. From Eq. (1) it can be seen that the PEC value of an effective enhancement technique should be at least larger than unity. The larger the PEC value, the better the overall thermo-hydraulic performance is. Meanwhile, it is also noted from Eq. (1) that a higher heat transfer rate does not mean a better overall performance. This tells us that full attention should be paid to flow resistance increase when developing a novel heat transfer augmentation technique.

Up to now, a variety of tube inserts have been developed by many researchers [4]. For instance, the twisted tape is the most widely used due to its steady performance, simple configuration and being easy to install and disassemble. The main mechanism for the heat transfer augmentation by applying a twisted tape is that it can generate swirls which enhance fluid mixing of the near-wall and central regions [5–8]. To improve the overall thermo-hydraulic performance of tubes fitted with twisted tapes, some modifications on the conventional twisted tape have been made. For example, segmented twisted tapes [9,10], broken twisted tapes [11], serrated twisted tape [12], center-cleared twisted tape [13],

* Corresponding author. Tel.: +86 27 87541998; fax: +86 27 87540724.
E-mail address: w_liu@hust.edu.cn (W. Liu).

0017-9310/$ - see front matter © 2012 Elsevier Ltd. All rights reserved.
http://dx.doi.org/10.1016/j.ijheatmasstransfer.2012.05.023

Nomenclature

c_p	the specific heat at constant pressure, kJ/kg K
D	the tube diameter, m
f	friction factor
h	the average heat transfer coefficient in the tube, W/m^2 K
k	turbulent kinetic energy, m^2/s^2
L	the full length of tube, m
L_0	the length of investigated region, m
L_1	the length before investigated region, m
L_2	the length after investigated region, m
Nu	average Nusselt number
p	pressure, N/m^2
q	heat transfer rate per unit tape length, W/m
Re	the Reynolds number
S	pitch of louvered strip, m
T	temperature, K
u	flow velocity in x direction, m/s
v	flow velocity in y direction, m/s
w	flow velocity in z direction, m/s

Greek symbols

α	slant angle (°)
β	field synergy angle between the flow and temperature gradient fields (°)
θ	field synergy angle between the flow and pressure gradient fields (°)
ρ	density of air, kg/m^3
λ	thermal conductivity, W/m K
ε	turbulent dissipation rate, m^2/s^3

Subscripts

0	plain tube
m	mean
w	wall

and helical screw-tape [14–16], etc. were proposed and investigated. Additionally, many other kinds of tube inserts were also designed and studied, such as coiled wire turbulators [17–19], circular rings [20], porous medium inserts [21,22], louvered-ring turbulators [23–25], conical strip inserts [26], etc. Some researchers even adopted the combination of two enhancement techniques [27–29].

Recently, Eiamsa-ard et al. [30] developed a louvered strip insert which looks like a leaf, only that the strip is planar. They experimentally investigated the effects of forward and backward arrangements, and inclined angle on the thermo-hydraulic performance of turbulent water flow. The results showed that the performance evaluation criterion (PEC) was around 1.17–1.98 for backward arrangement, and 1.11–1.8, for forward arrangement. However, they did not investigate the effect of the pitch of the louvered strip inserts. Also, the thermo-hydraulic performance of turbulent gas flow has not been reported yet. Therefore, in the present paper, we investigate the heat transfer and flow resistance characteristics of turbulent air flow in a circular tube fitted with the louvered strip inserts through numerical simulation. Our main attention will be paid to the effects of two parameters, i.e., the slant angle and pitch of the louvered strip inserts.

2. Numerical modeling

2.1. Physics model

A schematic of the physical model is shown in Fig. 1. The louvered strip is a planar leaf-shaped turbulator which connects with a central rod of 1 mm diameter. The length, width and thickness of the louvered strip are 16 mm, 10 mm and 1 mm, respectively. As demonstrated in [30], the backward arrangement has a higher PEC value as compared with that of the forward arrangement. Thus, we only adopt the backward arrangement in the present work. The effect of different combinations of the slant angle (α = 10°, 20° and 30°) and pitch (S = 30, 45 and 60 mm) will be investigated. The length and inner diameter of the tube are L = 500 mm and D = 19.6 mm, respectively. The length of the investigated region is $L0$ = 300 mm, with an upstream section of $L1$ = 100 mm and a downstream section of $L2$ = 100 mm. Air is selected as the working fluid. Heat conduction in the louvered strips and central rod is neglected. The thickness of solid wall is also not considered.

2.2. Governing equations

The problem under consideration is assumed to be three-dimensional, turbulent and steady. The following assumptions are made for the derivation of governing equations: (1) the physical properties of fluid are constant; (2) fluid is incompressible, isotropic and continuous; (3) fluid is Newtonian fluid; (4) the effect of gravity is negligible. Equations of continuity, momentum and energy for the fluid flow are given below in a tensor form.

Continuity equation:

$$\frac{\partial(\rho u_i)}{\partial x_i} = 0 \tag{2}$$

Momentum equation:

$$\frac{\partial}{\partial x_j}(\rho u_i u_j) = -\frac{\partial p}{\partial x_i} + \frac{\partial}{\partial x_j}\left[\mu\left(\frac{\partial u_i}{\partial x_j} + \frac{\partial u_j}{\partial x_i}\right)\right] \tag{3}$$

Energy equation:

$$\frac{\partial}{\partial x_j}\left(\rho u_j C_P T - k\frac{\partial T}{\partial x_j}\right) = u_j\frac{\partial p}{\partial x_j} + \left[\mu\left(\frac{\partial u_i}{\partial x_j} + \frac{\partial u_j}{\partial x_i}\right)\right] \tag{4}$$

In the present study, k–ε RNG turbulence model is used as follows:

$$\frac{\partial(\rho k)}{\partial t} + \frac{\partial(\rho k u_i)}{\partial x_i} = \frac{\partial}{\partial x_j}\left[\alpha_k \mu_{\text{eff}}\frac{\partial k}{\partial x_j}\right] + G_k - \rho\varepsilon \tag{5}$$

$$\frac{\partial(\rho\varepsilon)}{\partial t} + \frac{\partial(\rho\varepsilon u_i)}{\partial x_i} = \frac{\partial}{\partial x_j}\left[\alpha_k \mu_{\text{eff}}\frac{\partial \varepsilon}{\partial x_j}\right] + \frac{C^*_{1\varepsilon}\varepsilon}{k}G_k - C_{2\varepsilon}\rho\frac{\varepsilon^2}{k} \tag{6}$$

where ρ is the density of air; u, v, w refer to the flow velocities in x, y, z directions, respectively; c_p is the specific heat at constant pressure; λ is thermal conductivity; μ is dynamic viscosity; k is turbulent kinetic energy; ε is dissipation rate; In Eqs. (5) and (6), $\mu_{\text{eff}} = \mu + \mu_t$, $\mu_t = \rho C_\mu \frac{k^2}{\varepsilon}$, $C_\mu = 0.0845$, $\alpha_k = \alpha_\varepsilon = 1.39$, $C^*_{1\varepsilon} = C_{1\varepsilon} - \eta\left(1 - \frac{\eta}{\eta_0}\right)/(1 + \beta\eta^3)$, $C_{1\varepsilon} = 1.42$, $C_{2\varepsilon} = 1.68$, $\eta_0 = 4.377$, $\eta = (2E_{ij}\cdot E_{ij})^{1/2}\frac{k}{\varepsilon}$, $E_{ij} = \frac{1}{2}\left(\frac{\partial u_i}{\partial x_j} + \frac{\partial u_j}{\partial x_i}\right)$, $\beta = 0.012$.

To validate the CFD model, we take the case of Re = 19,692 as an example, and compare the experimental data in ref. [30] with our simulation results. The discrepancies of the Nusselt number (Nu) and overall thermo-hydraulic performance (PEC) are 2.4% and 4.0%, respectively. This verifies that the selection of the RNG k–ε model in our numerical simulation is reasonable.

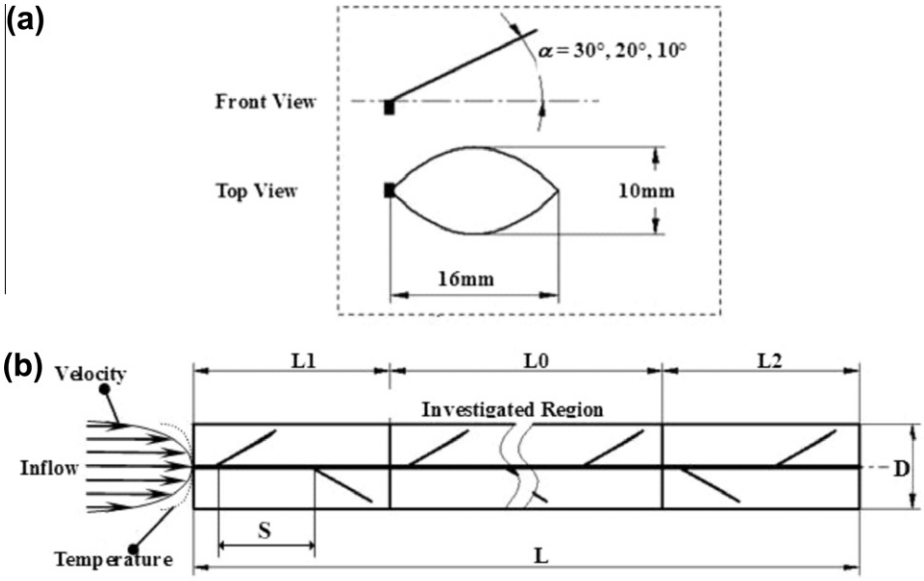

Fig. 1. (a) Geometry of the louvered strip insert, and (b) schematic of a circular tube fitted with louvered strip inserts.

2.3. Boundary conditions

The constant heat flux condition is specified on the tube wall. The enhanced wall function method was adopted for the treatment of tube wall and surfaces of louvered strips. At the tube inlet, fully developed flow and temperature boundary conditions are applied. The inlet velocity and temperature profiles were obtained via the following scheme. First, we used uniform inlet velocity and temperature profiles for the smooth tube and conducted one computation. Then, re-computation was performed using the outlet velocity and temperature profiles of the first time. After several times of computation applying this approach, fully developed flow and temperature profiles can be obtained. An example of Re = 24,000 is given in Fig. 2. From Fig. 2(a) it is clearly seen that the superposition of velocity profiles at the inlet and outlet of the tube are quite well. Meanwhile, after subtracting a constant (25.922 K), the temperature profile at the outlet matches very well with that at the inlet, as shown in Fig. 2(b).

At the outlet, a pressure-outlet condition is used. On the tube walls, and the surfaces of the louvered strips and central rod, no slip conditions are imposed.

2.4. Computation scheme and validation

Fig. 3 schematically shows the meshes generation of the computation domain. Rectangular and triangular cells were used to mesh the surfaces of tube wall and inserts, respectively; while for the internal space of the circular tube, tetrahedral meshes were adopted. Local grid refinement was applied in the boundary layers. Adaptive grid refinement was also performed in the preliminary computations. The grid independence has been checked by using different grid systems and around 2,000,000 grids are employed to conduct the following computations.

All the above-mentioned equations accompanied by boundary conditions are discretized using finite volume formulation. In the equations, the momentum, turbulent kinetic energy, turbulent dissipation rate and temperature terms are modeled by the second-order upwind scheme. The numerical solution procedure adopts the 'SIMPLE' algorithm. The convergent criterion is set as the relative residual of all variables to be less than 10^{-6}. The commercial CFD software package, Fluent 6.3, is used for the numerical simulation.

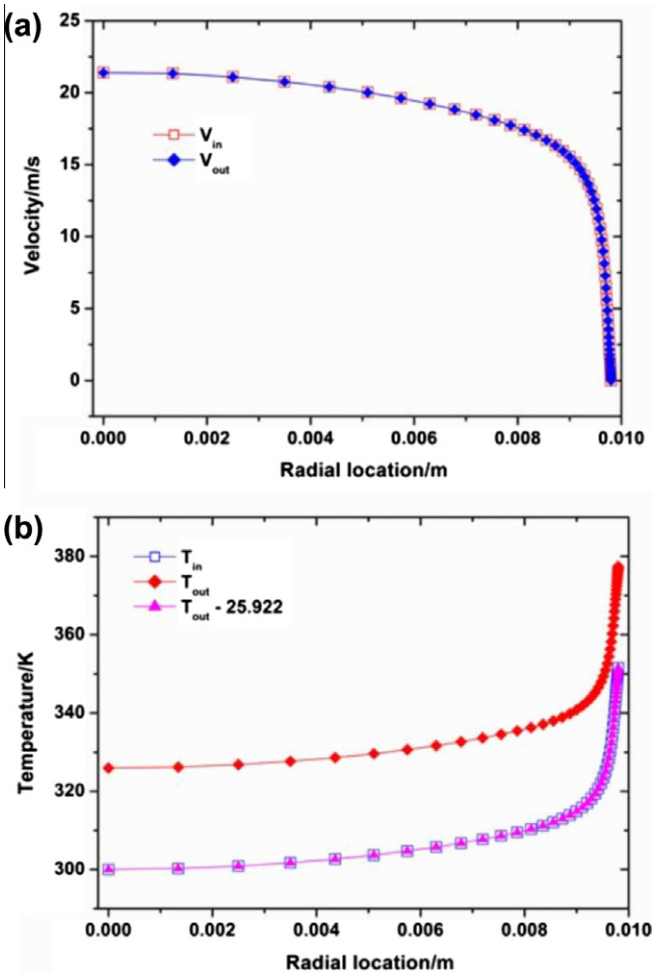

Fig. 2. Fully developed flow and temperature boundary conditions applied at the tube inlet: (a) velocity, and (b) temperature.

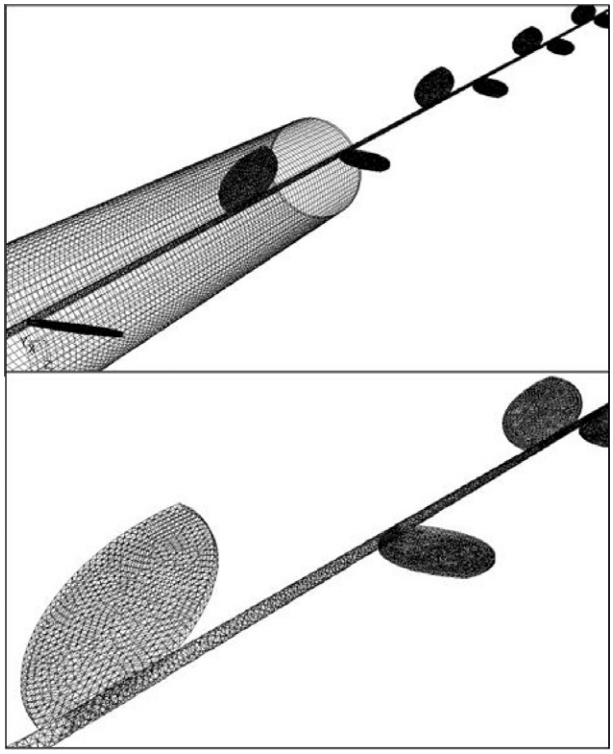

Fig. 3. Meshes generation of the computation domain.

To verify the numerical method described above, we compared the computational results with the well known empirical formulae for fully developed turbulent flows. From the comparison presented in Fig. 4, it is seen that the agreement between the CFD results and empirical correlations are fairly well. Therefore, the present numerical predictions have reasonable accuracy.

3. Results and discussion

3.1. Calculations of the Nusselt number, friction factor and PEC

After computing the velocity and temperature fields, heat transfer coefficient between the fluid and wall is calculated as

$$h = \frac{q}{T_w - T_m} \tag{7}$$

where T_m is bulk temperature of the fluid:

$$T_m = \frac{\int_0^R uTr\,dr}{\int_0^R ur\,dr} \tag{8}$$

The Nusselt number and friction factor can be calculated as

$$Nu = \frac{hD}{\lambda} \tag{9}$$

$$f = \frac{2\Delta PD}{L\rho u_m^2} \tag{10}$$

where u_m is the mean velocity of the transverse plane in the tube. ΔP could be determined by the difference between the mass-averaged pressures at the inlet and outlet of the investigated region.

To evaluate the effect of heat transfer enhancement under given pumping power, the performance evaluation criterion (PEC) is employed, as shown in Eq. (1).

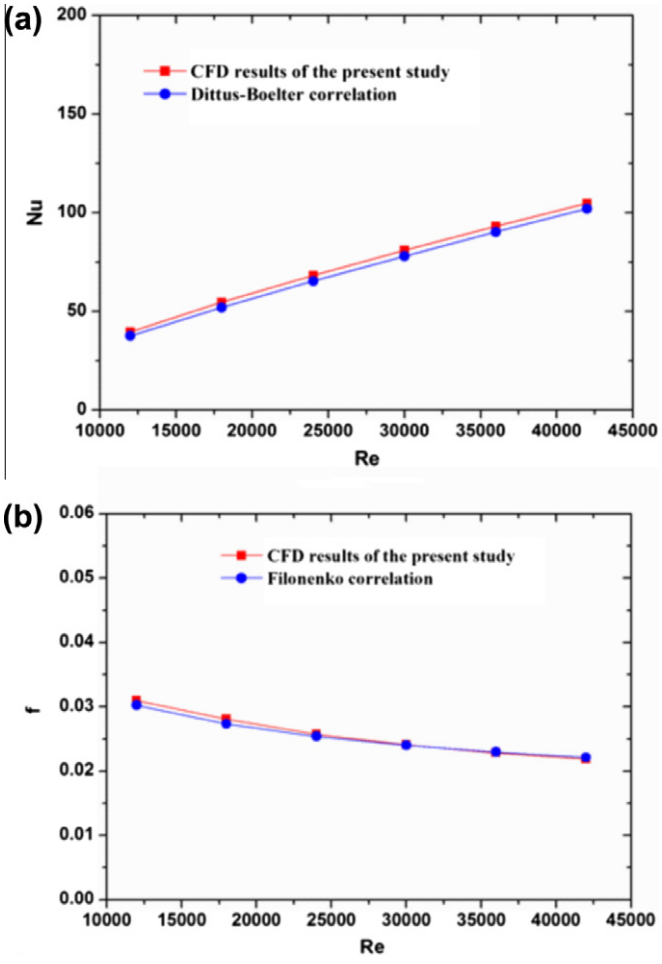

Fig. 4. Data verification of the Nusselt number *Nu* and friction factor *f* for smooth tube: (a) *Nu*, and (b) *f*.

3.2. Variation of the average Nusselt number

The variations of the average Nusselt number versus the Reynolds number are shown in Figs. 5–7 for louvered strip inserts with different pitches. It is noted that the average Nusselt number is augmented by around 2.45–4.05 times as that of the smooth tube.

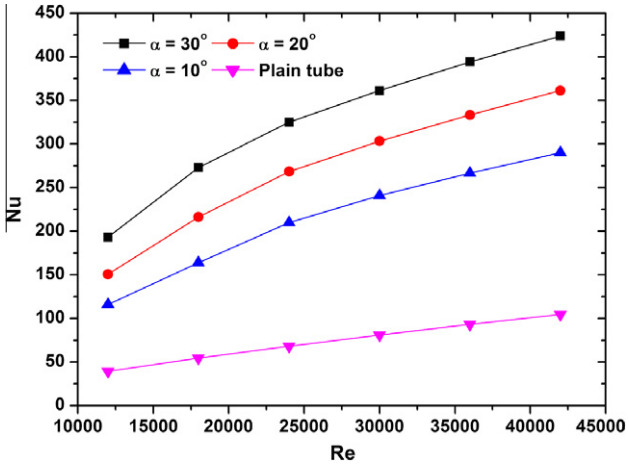

Fig. 5. Variation of the Nusselt number with Reynolds number for different slant angles. The pitch of the inserts is 30 mm in this case.

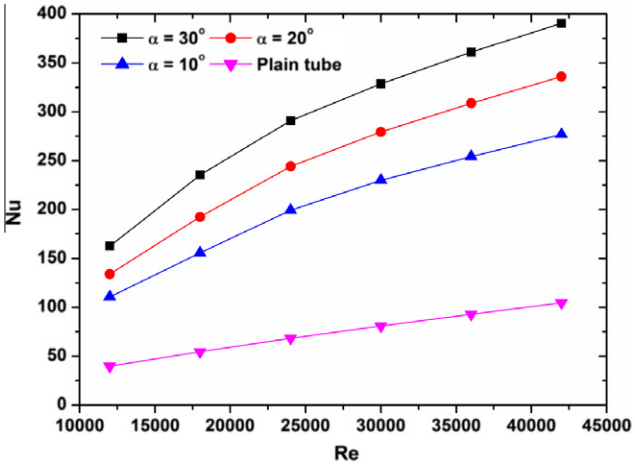

Fig. 6. Variation of the Nusselt number with Reynolds number for different slant angles. The pitch of the inserts is 45 mm in this case.

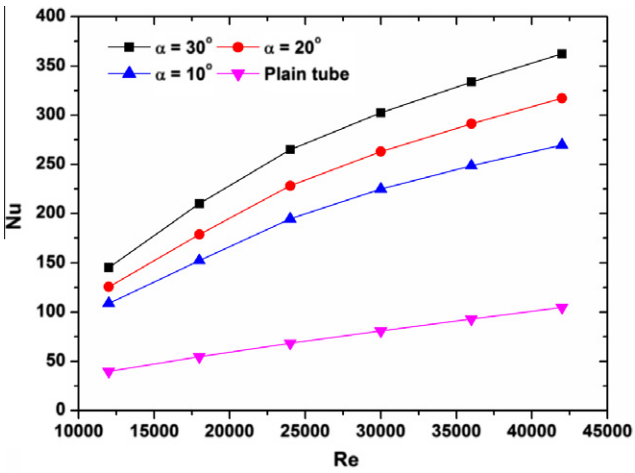

Fig. 7. Variation of the Nusselt number with Reynolds number for different slant angles. The pitch of the inserts is 60 mm in this case.

This verifies that the louvered strip has a good effect of heat transfer enhancement. Moreover, some general tendencies can be drawn from Figs. 5–7. First, the average Nusselt number increases with the increase of the Reynolds number. Second, the average Nusselt number increases with the increase of the slant angle of louvered strip when the Reynolds number and the inserts pitch are the same. In other words, the larger the slant angle, the higher the convective heat transfer rate is.

To facilitate examining the effect of inserts pitch on the heat transfer enhancement, we plot all those data in Fig. 8. From this figure, one can see that when the slant angle is 30°, a relatively small pitch has a much better effect on heat transfer enhancement, which is clearly illustrated by the three red lines in Fig. 8. However, with the decrease of the slant angle ($\alpha = 20°$), the impact of inserts pitch grows not so significant. When $\alpha = 10°$, the influence of inserts pitch becomes very limited, as shown in Fig. 8.

3.3. Variation of the friction factor

Figs. 9–11 depict the variations of the friction factor versus the Reynolds number for louvered strip inserts of different pitches. It is noted that the friction factor of the enhanced tube is about 3.9–16.2 times that of the smooth tube. Contrast with the Nusselt number, the friction factor decreases with the increase of the Reynolds

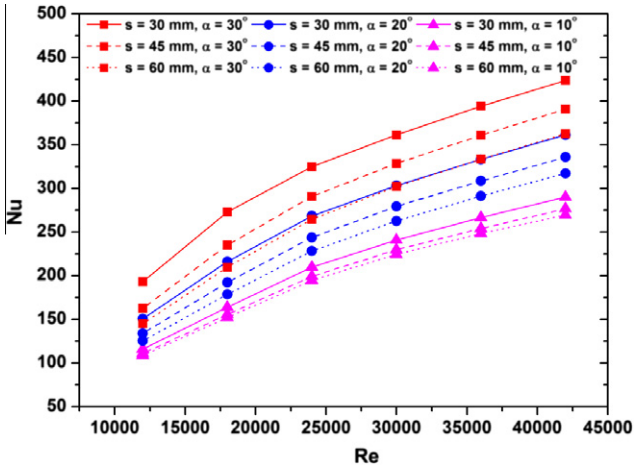

Fig. 8. Variation of the Nusselt number with Reynolds number for different slant angles and pitches.

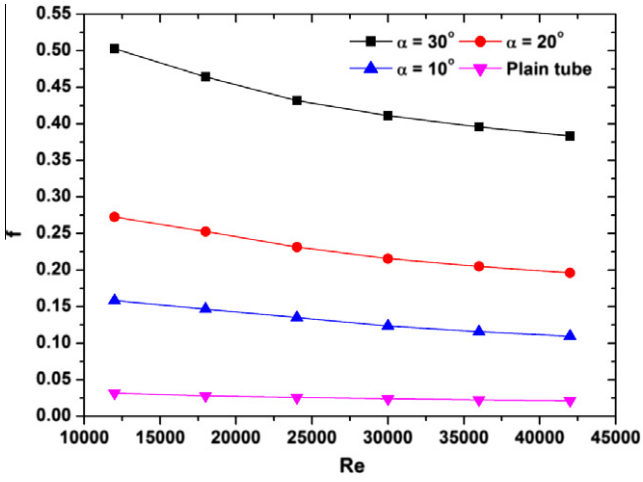

Fig. 9. Variation of the friction factor with Reynolds number for different slant angles. The pitch of the inserts is 30 mm in this case.

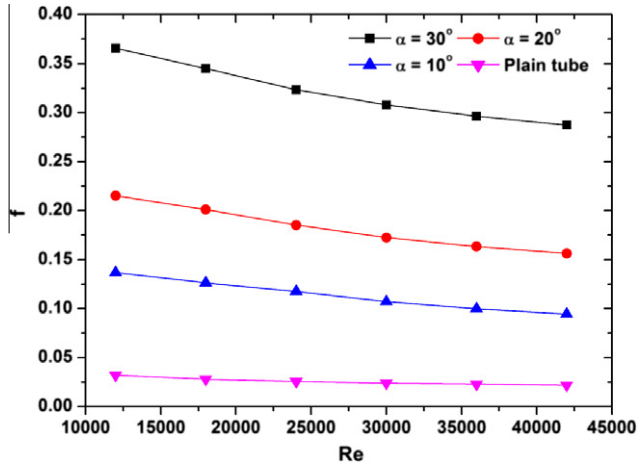

Fig. 10. Variation of the friction factor with Reynolds number for different slant angles. The pitch of the inserts is 45 mm in this case.

number. Moreover, the friction factor increases with the increase of the slant angle of louvered strip when the Reynolds number and inserts pitch are the same. In other words, the larger the slant

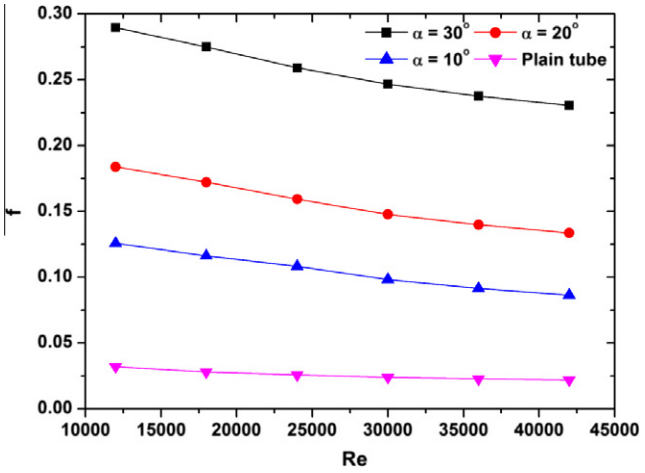

Fig. 11. Variation of the friction factor with Reynolds number for different slant angles. The pitch of the inserts is 60 mm in this case.

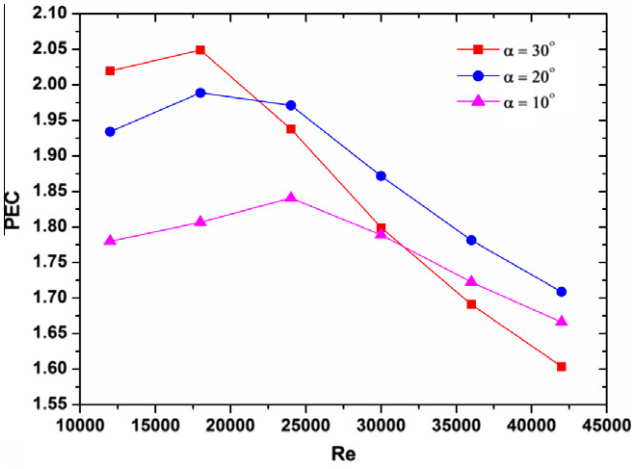

Fig. 13. Variation of the PEC value with Reynolds number for different slant angles. The pitch of the inserts is 30 mm in this case.

angle, the larger the flow resistance is. This variation tendency is the same as that of the Nusselt number.

Similarly, for convenience of examining the effect of inserts pitch on the friction factor, we put all the data of Figs. 9–11 in Fig. 12. From this figure, one can see that when the slant angle is 30°, a relatively small pitch results in a much larger friction factor, which is clearly illustrated by the three red lines in Fig. 12. However, with the decrease of the slant angle ($\alpha = 20°$), the impact of inserts pitch is also reduced. When $\alpha = 10°$, the influence of inserts pitch is very weak, as shown in Fig. 12.

3.4. Variation of the performance evaluation criterion (PEC)

The variation tendencies of performance evaluation criterion (PEC) versus the Reynolds number are shown in Figs. 13–15 for louvered trip inserts of different pitches. From these figures it is seen that the PEC value lies in the range of 1.60–2.05, which demonstrates that the louvered strip insert has a very good thermo-hydraulic performance. Different from the Nusselt number and friction factor, the variation of PEC is not monotonically. In other words, it first increases with the increase of the Reynolds number, and then decreases with the further increase of the Reynolds number. At a moderate *Re*, the PEC reaches its peak value. Furthermore, the PEC of a relatively small pitch decreases more quickly when the

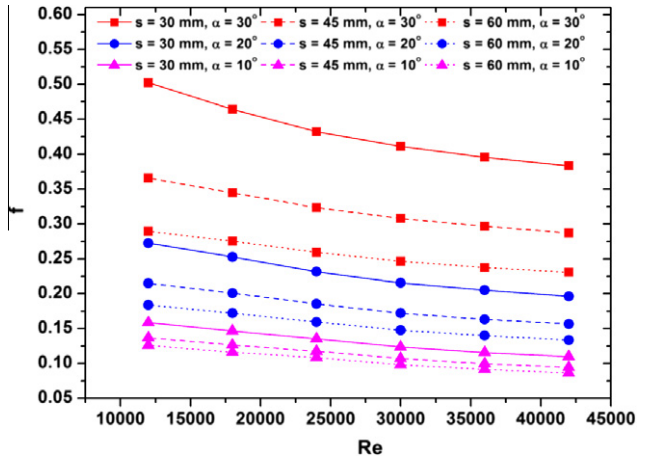

Fig. 12. Variation of the friction factor with Reynolds number for different slant angles and pitches.

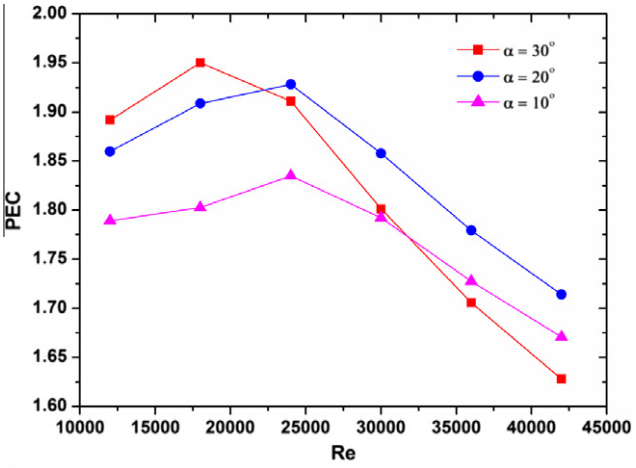

Fig. 14. Variation of the PEC value with Reynolds number for different slant angles. The pitch of the inserts is 45 mm in this case.

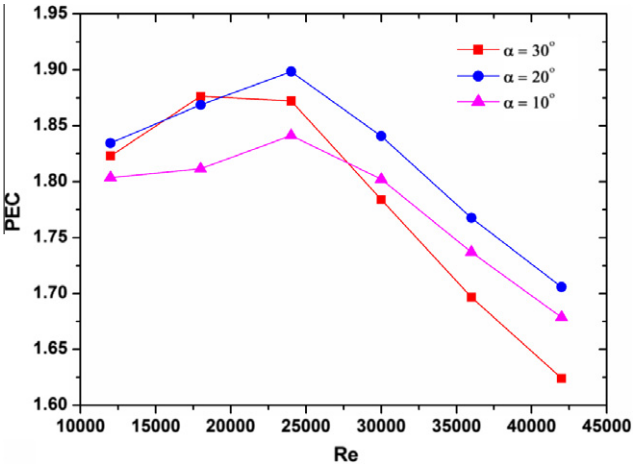

Fig. 15. Variation of the PEC value with Reynolds number for different slant angles. The pitch of the inserts is 60 mm in this case.

Reynolds number is larger than its critical value. Thus, under large *Re* conditions, the PEC of the case with a small pitch can drop to a value less than that of a large pitch, as shown in Figs. 13–15.

To reveal the reason for the non-monotonic variation tendency of PEC, we examined the plots of Nu/Nu_0 and $(f/f_0)^{1/3}$ with Reynolds number, although not presented here. It is shown that Nu/Nu_0 reaches its peak value at a moderate *Re*, while the variation of $(f/f_0)^{1/3}$ is very small. Therefore, the variation tendency of PEC is accordance with that of Nu/Nu_0.

Fig. 16 depicts all the data in Figs. 13–15. From this figure it is clearly seen that when the Reynolds number is small, a better thermo-hydraulic performance can be achieved by using a larger slant angle ($\alpha = 30°$) together with a relatively small pitch ($S = 30$ and 45 mm). However, when the Reynolds number is large, a moderate slant angle ($\alpha = 20°$) together with a short pitch ($S = 30$ mm) should be selected to obtain a largest PEC value. Meanwhile, the PEC values of this combination ($\alpha = 20°$ and $S = 30$ mm) are also relatively high at low *Re*. Thus, to achieve a relatively good thermo-hydraulic performance over the whole *Re* range, the best parameter combination should be $\alpha = 20°$ and $S = 30$ mm.

For comparison, we also present the PEC values of continuous twisted tape [7] and broken twisted tape [11] in Fig. 16. It is evident that the PEC values of continuous twisted tape are less than unity in the turbulent flow regime. Although the thermo-hydraulic performance has been improved to some extent in the case of broken twisted tape, the PEC values are still much lower than the counterparts of the louvered strip insert. This demonstrates that the louvered strip insert has a very good thermo-hydraulic performance in the turbulent flow regime.

3.5. Discussions

The numerical results demonstrated that the heat transfer rate and flow resistance depend on the parameters combination of the louvered strip. This is because the fluid mixing, boundary layer disturbing, and convective heat transfer have close relation to those geometric parameters. Thus, we present the flow and temperature fields of the case at *Re* = 24,000 as example to analyze the effect of the geometric parameters, as shown in Figs. 17 and 18, respectively. From Fig. 17(a)–(c), it is clearly seen that the fluid mixing and boundary disturbing are greatly intensified when the slant angle of the louvered strip is increased from 10° to 30°. Thus, the flow boundary layer becomes thinner at larger slant angles. This will result in a significant increase in the friction factor, as have been shown in Figs. 9–12. Similarly, due to the good effect of fluid mixing and boundary disturbing at large slant angle, the temperature field grows more uniform in the core flow region, and the temperature gradient becomes larger in the boundary layer simultaneously. Therefore, heat transfer will be substantially enhanced and the outlet temperature will be higher at large slant angles of the louvered strip.

It is well known that flow and heat transfer have interaction on each other in convective heat transfer processes, therefore, thermal augmentation has a relationship to the distributions of both velocity and temperature fields. In the past decade, the field synergy theory was first proposed by Guo et al. [31–33], further developed by Tao et al. [34,35] and Liu et al. [36–39], and applied by other

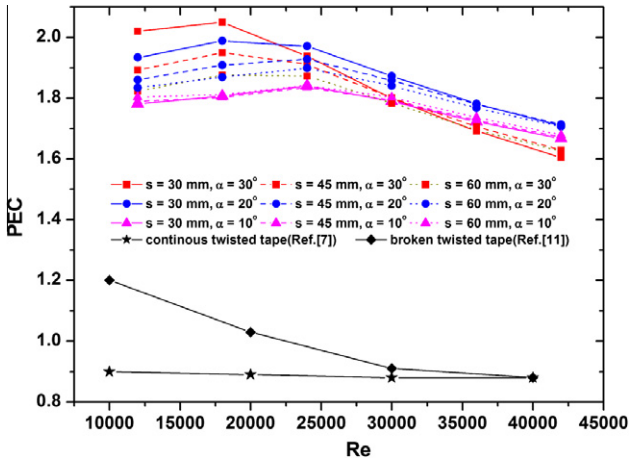

Fig. 16. Variation of the PEC value with Reynolds number for louvered strip inserts of different slant angles and pitches. For comparison, PEC values of continuous [7] and broken [11] twisted tapes are also presented here.

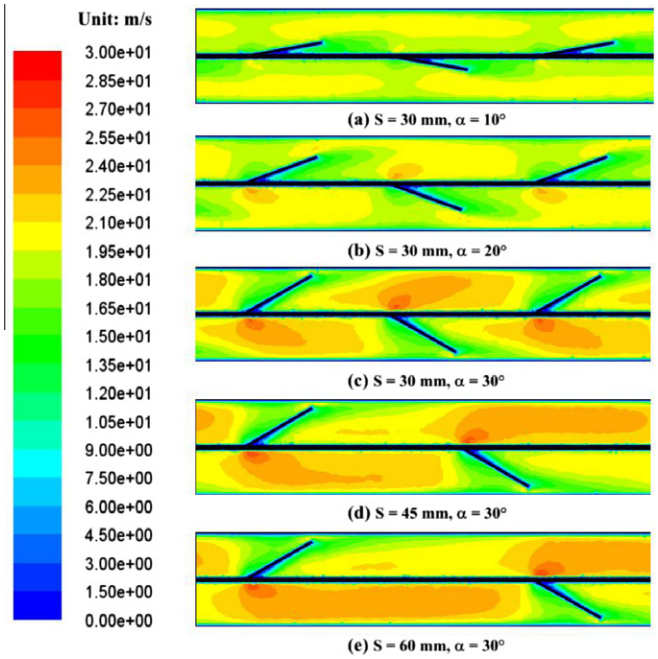

Fig. 17. Velocity contours at *Re* = 24,000: (a) $S = 30$ mm, $\alpha = 10°$, (b) $S = 30$ mm, $\alpha = 20°$, (c) $S = 30$ mm, $\alpha = 30°$, (d) $S = 45$ mm, $\alpha = 30°$, and (e) $S = 60$ mm, $\alpha = 30°$.

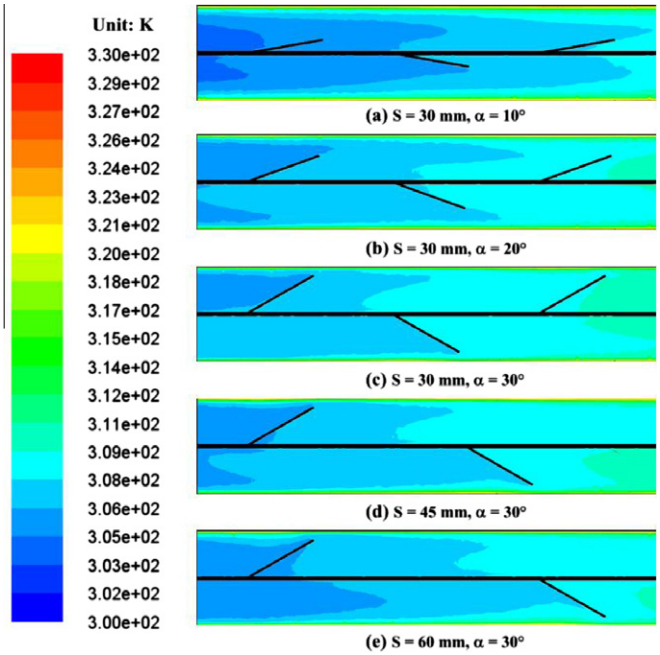

Fig. 18. Temperature contours at *Re* = 24,000: (a) $S = 30$ mm, $\alpha = 10°$, (b) $S = 30$ mm, $\alpha = 20°$, (c) $S = 30$ mm, $\alpha = 30°$, (d) $S = 45$ mm, $\alpha = 30°$, and (e) $S = 60$ mm, $\alpha = 30°$.

researchers for heat exchanger optimization design [40]. This principle indicates that in a convective heat transfer process, the heat transfer rate depends not only on the magnitudes of the flow velocity and temperature gradient (driving force of the heat transfer) but also on their synergy [31–35]. Similarly, the flow resistance closely relates to the coordination between the flow field and pressure gradient (driving force of the flow) field [36–39]. Therefore, synergy angles β and θ were proposed to evaluate and help analyzing the thermal and hydraulic performances of a heat transfer process. The definitions of those two synergy angles are given in Eqs. (11) and (12), respectively [31–39].

$$\beta = \arccos\frac{U\cdot\nabla T}{|U||\nabla T|} \tag{11}$$

$$\theta = \arccos\frac{U\cdot\nabla p}{|U||\nabla p|} \tag{12}$$

According to the field synergy principle, the better the coordination between the velocity and temperature gradient fields, the higher the convective heat transfer rate is; while the better the coordination between the velocity and pressure gradient fields, the lower the flow resistance is. More specifically, a smaller β means a higher heat transfer rate (a larger Nu); while a smaller θ means a lower flow resistance (a smaller f), providing that those synergy angles are acute angles (i.e., less than 90°).

For the present study, the underlying physics of the effects of the slant angle on the Nusselt number and friction factor can be further explained by the field synergy theory. Figs. 19 and 20 give an example of the synergy angles, β and θ, at different slant angles of the louvered strip inserts when the pitch is 30 mm. It is clearly shown in Fig. 19 that when the slant angle of the inserts is larger, the synergy angle, β, is smaller, which implies that a larger Nusselt number can be obtained. This qualitatively well agrees with the variation tendency of Nu presented in Fig. 5. The mechanism is that a larger slant angle can change the flow direction more significantly to the radial direction (i.e., produce a larger radial velocity component), which can disturb the boundary layer more intensively. Similarly, it is evident from Fig. 20 that when the slant angle of the inserts is larger, the synergy angle, θ, is also larger. This implies that the coordination between the velocity and pressure gradient fields becomes worse, which leads to a larger fiction factor. This is consistent with the variation tendency of f shown in Fig. 9.

Explanation of the effect of inserts pitch is relatively simple. When the inserts pitch is small, more insert elements could be added into the investigated region, as shown in Fig. 17(c)–(e) and Fig. 18(c)–(e). Thus, both the flow resistance and heat transfer rate will be increased.

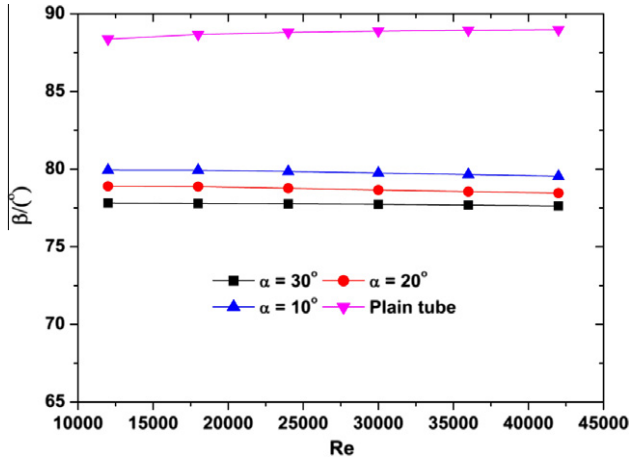

Fig. 19. The field synergy angle (β) between the flow field and temperature gradient field. The pitch of the louvered strip inserts is 30 mm.

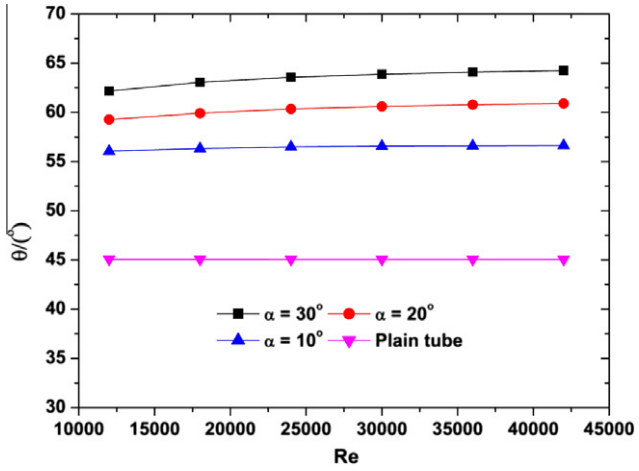

Fig. 20. The field synergy angle (θ) between the flow field and pressure gradient field. The pitch of the louvered strip inserts is 30 mm.

As for the PEC value, its variation tendency is more complex. This is because it depends on the Nusselt number and friction factor of the enhanced tube and smooth tube simultaneously. In more details, the PEC value is proportional to the ratio, Nu/Nu_0, and inversely proportional to the ratio $(f/f_0)^{1/3}$. From Figs. 8 and 12, we have already known that the Nusselt number and friction factor are more sensitive to the slant angle than the inserts pitch. Therefore, comparatively steady and good overall thermo-hydraulic performance is obtained at a moderate slant angle ($\alpha = 20°$) together with a small pitch ($S = 30$ mm).

4. Conclusions

Characteristics of the Nusselt number, friction factor, and performance evaluation criterion of turbulent flow in a circular tube fitted with louvered strip inserts were investigated through numerical simulation. The computation results show that the Nusselt number is augmented by around 4 times that of the smooth tube, which confirms that the louvered strip has a good effect of heat transfer enhancement. The PEC value lies in the range of 1.60–2.05, which demonstrates that the louvered strip insert has a very good overall thermo-hydraulic performance.

Effects of the geometric parameters of the louvered strip were examined. The numerical results indicate that: (1) larger slant angle and small pitch can effectively enhance the heat transfer rate, but also increase the flow resistance. This is due to the higher turbulence intensity; (2) the Nusselt number and friction factor are more sensitive to the slant angle than the inserts pitch, because a larger slant angle can produce a larger radial flow velocity; (3) comparatively steady and good overall thermo-hydraulic performance is obtained at a moderate slant angle ($\alpha = 20°$) together with a small pitch ($S = 30$ mm), which is a tradeoff between the heat transfer enhancement and flow resistance increase.

In addition to those good performances, the louvered strip is also easy to fabricate. Thus, it is a promising tube insert which can be widely used in heat transfer enhancement of turbulent flow.

Acknowledgements

This work was supported by the Natural Science Foundations of China (Nos. 51036003 and 51076054) and the Doctoral Fund of Ministry of Education of China (No. 20100142110037).

References

[1] A.E. Bergles, ExHFT for fourth generation heat transfer technology, Experimental Thermal and Fluid Science 26 (2002) 335–344.
[2] V. Zimparov, Energy conservation through heat transfer enhancement techniques, International Journal of Energy Research 26 (2002) 675–696.
[3] R.L. Webb, Performance evaluation criteria for use of enhanced heat transfer surfaces in heat exchanger design, International Journal of Heat and Mass Transfer 24 (1981) 715–726.
[4] L. Wang, B. Sunden, Performance comparison of some tube inserts, International Communications in Heat and Mass Transfer 29 (2002) 45–56.
[5] P. Naphon, Heat transfer and pressure drop in the horizontal double pipes with and without twisted tape insert, International Communications in Heat and Mass Transfer 33 (2006) 166–175.
[6] R.M. Manglik, A.E. Bergles, Heat transfer and pressure drop correlations for twisted tape inserts in isothermal tubes: Part I – laminar flows, Journal of Heat Transfer 115 (1993) 881–889.
[7] R.M. Manglik, A.E. Bergles, Heat transfer and pressure drop correlations for twisted tape inserts in isothermal tubes: Part II – transition and turbulent flows, Journal of Heat Transfer 115 (1993) 890–896.
[8] A. Kumar, B.N. Prasad, Investigation of twisted tape inserted solar water heaters – heat transfer, friction factor and thermal performance results, Renewable Energy 19 (2000) 379–398.
[9] S.K. Saha, A. Dutta, S.K. Dhal, Friction and heat transfer characteristics of laminar swirl flow through a circular tube fitted with regularly spaced twisted-tape elements, International Journal of Heat and Mass Transfer 44 (2001) 4211–4223.
[10] S. Eiamsa-ard, C. Thianpong, P. Promvonge, Experimental investigation of heat transfer and flow friction in a circular tube fitted with regularly spaced twisted tape elements, International Communications in Heat and Mass Transfer 33 (2006) 1225–1233.
[11] S.W. Chang, T.L. Yang, J.S. Liou, Heat transfer and pressure drop in tube with broken twisted tape insert, Experimental Thermal and Fluid Science 32 (2007) 489–501.
[12] S.W. Chang, Y.J. Jan, J.S. Liou, Turbulent heat transfer and pressure drop in tube fitted with serrated twisted tape, International Journal of Thermal Science 46 (2007) 506–518.
[13] J. Guo, A.W. Fan, X.Y. Zhang, W. Liu, A numerical study on heat transfer and friction factor characteristics of laminar flow in a circular tube fitted with center-cleared twisted tape, International Journal of Thermal Science 50 (2011) 1263–1270.
[14] P. Sivashanmugam, S. Suresh, Experimental studies on heat transfer and friction factor characteristics of laminar flow through a circular tube fitted with helical screw-tape inserts, Applied Thermal Engineering 26 (2006) 1990–1997.
[15] P. Sivashanmugam, S. Suresh, Experimental studies on heat transfer and friction factor characteristics of turbulent flow through a circular tube fitted with regularly spaced helical screw-tape inserts, Applied Thermal Engineering 27 (2007) 1311–1319.
[16] S. Eiamsa-ard, P. Promvonge, Enhancement of heat transfer in a tube with regularly-spaced helical tape swirl generators, Solar Energy 78 (2005) 483–494.
[17] P. Promvonge, Thermal performance in circular tube fitted with coiled square wires, Energy Conversion and Management 49 (2008) 980–987.
[18] A. Carcia, J.P. Solano, P.G. Vicente, A. Viedma, Enhancement of laminar and transitional flow in tubes by means of wire coil inserts, International Journal of Heat and Mass Transfer 50 (2007) 3176–3189.
[19] K. Yakut, B. Sahin, The effects of vortex characteristics on performance of coiled wire turbulators used for heat transfer augmentation, Applied Thermal Engineering 24 (2004) 2427–2438.
[20] V. Ozceyhan, S. Gunes, O. Buyukalaca, N. Altuntop, Heat transfer enhancement in a tube using circular cross sectional rings separated from wall, Applied Energy 85 (2008) 988–1001.
[21] S.O. Akansu, Heat transfers and pressure drops for porous-ring turbulators in a circular pipe, Applied Energy 83 (2006) 280–298.
[22] Z.F. Huang, A. Nakayama, K. Yang, C. Yang, W. Liu, Enhancing heat transfer in the core flow by using porous medium insert in a tube, International Journal of Heat and Mass Transfer 53 (2010) 1164–1174.
[23] K. Yakut, B. Sahin, Flow-induced vibration analysis of louvered rings used for heat transfer enhancement in heat exchangers, Applied Energy 78 (2004) 273–288.
[24] K. Yakut, B. Sahin, C. Celik, S. Canbazoglu, Performance and flow-induced vibration characteristics for louvered-ring turbulators, Applied Energy 79 (2004) 65–76.
[25] P. Promvonge, Heat transfer behaviors in round tube with louvered ring inserts, Energy Conversion and Management 49 (2008) 8–15.
[26] A.W. Fan, J.J. Deng, J. Guo, W. Liu, A numerical study on thermo-hydraulic characteristics of turbulent flow in a circular tube fitted with conical strip inserts, Applied Thermal Engineering 31 (2011) 2819–2828.
[27] P. Promvonge, Thermal augmentation in circular tube with twisted tape and wire coil turbulators, Energy Conversion and Management 49 (2008) 2949–2955.
[28] P. Promvonge, S. Eiamsa-ard, Heat transfer enhancement in a tube with combined louvered-nozzle inserts and swirl generator, Energy Conversion and Management 47 (2006) 2867–2882.
[29] P. Promvonge, S. Eiamsa-ard, Heat transfer behaviors in a tube with combined louvered-ring and twisted-tape insert, International Communications in Heat and Mass Transfer 34 (2007) 849–859.
[30] S. Eiamsa-ard, S. Pethkool, C. Thianpong, P. Promvonge, Turbulent flow heat transfer and pressure loss in a double pipe heat exchanger with louvered strip inserts, International Communications in Heat and Mass Transfer 35 (2008) 120–129.
[31] Z.Y. Guo, D.Y. Li, B.X. Wang, A novel concept for convective heat transfer enhancement, International Journal of Heat and Mass Transfer 41 (1998) 2221–2225.
[32] Z.Y. Guo, Mechanics and control of convective heat transfer-coordination of velocity and heat flow fields, Chinese Science Bulletin 46 (2001) 597–600.
[33] Z.Y. Guo, W.Q. Tao, R.K. Shah, The field synergy principle and its applications in enhancing single phase convective heat transfer, International Journal of Heat and Mass Transfer 48 (2005) 1797–1807.
[34] W.Q. Tao, Z.Y. Guo, B.X. Wang, Field synergy principle for enhancing convective heat transfer-its extension and numerical verification, International Journal of Heat and Mass Transfer 45 (2002) 3849–3856.
[35] W.Q. Tao, Y.L. He, Z.G. Qu, Y.P. Cheng, Application of the field synergy principle in developing new type heat transfer enhanced surfaces, Journal of Enhanced Heat Transfer 11 (2004) 433–449.
[36] W. Liu, Z.C. Liu, et al., Physical quantity synergy in laminar flow field and its application in heat transfer enhancement, International Journal of Heat Mass Transfer 52 (2009) 4669–4672.
[37] W. Liu, Z.C. Liu, Z.Y. Guo, Physical quantity synergy in laminar flow field of convective heat transfer and analysis of heat transfer enhancement, Chinese Science Bulletin 54 (2009) 3579–3586.
[38] W. Liu, Z.C. Liu, S.Y. Huang, Physical quantity synergy in the field of turbulent heat transfer and its analysis for heat transfer enhancement, Chinese Science Bulletin 55 (2010) 2589–2597.
[39] W. Liu, Z.C. Liu, L. Ma, Application of a multi-field synergy principle in the performance evaluation of convective heat transfer enhancement in a tube, Chinese Science Bulletin 57 (13) (2012) 1600–1607.
[40] J.F. Guo, M.T. Xu, L. Cheng, The application of field synergy number in shell-and-tube heat exchanger optimization design, Applied Energy 86 (2009) 2079–2087.